

Document downloaded from the institutional repository of the University of Alcalá: <http://dspace.uah.es/dspace/>

This is the peer reviewed version of the following article: Pascual, G. et al. (2012) 'Effects of collagen prosthesis cross-linking on long-term tissue regeneration following the repair of an abdominal wall defect', *Wound repair and regeneration*, 20(3), pp. 402–413.

Which has been published in final form at:

<https://doi.org/10.1111/j.1524-475X.2012.00781.x>

This article may be used for non-commercial purposes in accordance with Wiley Terms and Conditions for Use of Self-Archived Versions. This article may not be enhanced, enriched or otherwise transformed into a derivative work, without express permission from Wiley or by statutory rights under applicable legislation. Copyright notices must not be removed, obscured or modified. The article must be linked to Wiley's version of record on Wiley Online Library and any embedding, framing or otherwise making available the article or pages thereof by third parties from platforms, services and websites other than Wiley Online Library must be prohibited.



This work is licensed under a  
Creative Commons Attribution-NonCommercial-NoDerivatives  
4.0 International License.

*(Article begins on next page)*



Universidad  
de Alcalá



This work is licensed under a  
Creative Commons Attribution-NonCommercial-NoDerivatives  
4.0 International License.

## **Effects of collagen prosthesis cross-linking on long-term tissue regeneration following the repair of an abdominal wall defect**

Gemma Pascual, PhD<sup>1,3</sup>; Marta Rodríguez, PhD<sup>2,3</sup>; Sandra Sotomayor, PhD<sup>2,3</sup>; Eduardo Moraleda, MD<sup>2</sup>; Juan M. Bellón, MD, PhD<sup>2,3</sup>

1. Department of Medical Specialities, University of Alcalá, Madrid, Spain

2. Department of Surgery, Faculty of Medicine, University of Alcalá, Madrid, Spain, and

3. Networking Research Center on Bioengineering, Biomaterials and Nanomedicine (CIBER-BBN), Madrid, Spain

### **ABSTRACT**

Collagen prostheses used to repair abdominal wall defects, depending on their pretreatment (noncross-linked vs. cross-linked), besides repair may also achieve tissue regeneration. We assessed the host tissue incorporation of different bioprostheses using a new tool that combines immunofluorescence confocal microscopy with differential interference contrast images, making it possible to distinguish newly formed collagen. Partial hernial defects in the abdominal wall of rabbits were repaired using cross-linked/noncross-linked bioprostheses. Expanded polytetrafluoroethylene (ePTFE) was used as control. After 14/30/90/180 days of implant, specimens were taken for microscopy, immunohistochemistry, and quantitative-reverse transcription-polymerase chain reaction to determine host tissue ingrowth and collagen I/III protein and 1a1/3a1 gene expression. Shrinkage and stress resistance were also examined. At 14 days, cross-linked prostheses had suffered significantly less shrinkage than ePTFE or noncross-linked prostheses. Significantly higher shrinkage was recorded for ePTFE in the longer term. Microscopy revealed encapsulation of ePTFE by neofomed tissue, while the bioprostheses became gradually infiltrated by host tissue. Noncross-linked prosthesis showed better tissue ingrowth, more intense inflammatory reaction and more rapid degradation than the cross-linked prostheses. At 14 days, cross-linked prostheses induced up-regulated collagen 1a1 and 3a1 gene expression, while noncross-linked only showed increased collagen III protein expression at 90 days postimplant. At 6 months, the tensile strengths of cross-linked prostheses were significantly greater compared with ePTFE. Our findings demonstrate that despite the cross-linked collagen prostheses promoting less tissue ingrowth than the noncross-linked meshes, they became gradually replaced by good quality host tissue and were less rapidly degraded, leading to improved stress resistance in the long term.

### **Reprint requests:**

Dr. J. M. Bellón, Department of Surgery, Faculty of Medicine, University of Alcalá, Ctra. Madrid-Barcelona Km 33,600, 28871Alcalá de Henares, Madrid, Spain.

Tel: +34 91 885 45 40;

Fax: +34 91 885 48 85;

Email: [juanm.bellon@uah.es](mailto:juanm.bellon@uah.es)

Manuscript received: June 1, 2011 Accepted in final form: January 20, 2012

DOI:10.1111/j.1524-475X.2012.00781.x

Coll	CollaMend®
DIC	Differential interference contrast
ePTFE	Expanded polytetrafluoroethylene
HDMI	Hexamethylene-di-isocyanate
Pe	Permacol®
SIS	Surgisis®

Modern hernia surgery is no longer imaginable without the use of a surgical mesh, with millions implanted each year for this purpose worldwide.<sup>1</sup>

To the materials available today for the repair of a hernial defect in the abdominal wall, we would have to add the new biological prosthetic materials.<sup>2</sup> Such materials derived from biological sources share the important feature that they are degraded and fully eliminated in the host<sup>3,4</sup> contrasting with the synthetic polymer materials that, once implanted, remain over a lifetime in the host and give rise to inflammatory and foreign body reactions leading to postimplant complications.<sup>5,6</sup> The gradual degradation of a biological prosthesis in the host will condition the formation in its place of a neotissue, which in the long term will completely replace the biomaterial. The goal is to induce the growth of an organized tissue that will promote angiogenesis and even recruit growth factors acquiring characteristics similar to those of healthy tissue.<sup>7</sup>

To accomplish this goal, degradation/regeneration needs to take place in a controlled fashion. This control is obtained by pretreating these biological prostheses with different substances (glutaraldehyde, hexamethylene di-isocyanate) that are able to stabilize these materials in an environment in which the collagenases present may quickly degrade them. Pretreatment produces cross-links that make the triple helix structure of collagen more solid avoiding its rapid degradation.<sup>8</sup>

Clinical experience in the use of biological prostheses is still limited for several reasons. First, inert materials exist (polypropylene, polyester, and expanded polytetrafluoroethylene [ePTFE]) that have provided good outcomes in patients, but they do not permit incorporation of host tissue;<sup>9,10</sup> second, biological meshes have precise indications for use in zones compromised by infection;<sup>11,12</sup> and third, these materials are expensive.<sup>13</sup>

In this study, we assess the use of three biological prosthetic materials of clinical use. All are derived from pig, one is cross-link free (Surgisis® [Cook, Limerick, Ireland]) and the others are cross-linked (Permacol® [Covidien, Dublin, Ireland] and CollaMend® [Bard, Murray Hill, NJ]). As a control, we used ePTFE, Preclude® (Gore, Flagstaff, AZ), as a prototype nonporous, laminar implant.

The main objective of our study was to gain insight into the host tissue incorporation process induced by the prosthetic meshes, mainly in terms of their collagenization. For this purpose, we designed a new analysis tool by combining immunofluorescence confocal microscopy with differential interference contrast (DIC) images. Using this procedure, we can differentiate the native collagen that forms the biological prostheses from the newly formed collagen in the regenerated tissue. This enables us to follow prosthetic material degradation and its replacement with newly formed host tissue over time. To determine which of the meshes would be best at inducing a neotissue of adequate characteristics, collagen deposition was also correlated with prosthetic

shrinkage and the biomechanical response in the implant zone.

## **MATERIALS AND METHODS**

### **Experimental animals**

The experimental animals were 40 male New Zealand White rabbits, weighing approximately 3,500 g. The study protocol was approved by our institution's review board. Throughout the study, the animals were caged under conditions of constant light and temperature. Housing, handling, experimental procedures, anesthesia, and euthanasia have been carried out according to European Union animal care guidelines (EEC 2871-22 A9).

### **Prosthetic materials**

The three collagen meshes tested were: two different cross-linked porcine dermal collagen implants, CollaMend (Coll) and Permacol (Pe), treated with 1-ethyl-3-(3-dimethylaminopropyl) carbodiimide (EDC) and HMDI, respectively, and Surgisis (SIS), a noncross-linked biologic prosthesis created from porcine small intestinal submucosa. Preclude (ePTFE), a laminar-structure ePTFE prosthesis, was used as control.

### **Experimental design**

The 40 experimental animals were implanted with two different meshes each (Coll/Pe or ePTFE/SIS), one on the right side and the other on the left side of the abdominal wall (Figure 1). Twenty animals were implanted with Coll/Pe and the remaining 20 with ePTFE/SIS. At each of the time points 14, 30, 90, and 180 days, 10 animals were euthanized (five implanted with Coll/Pe and five implanted with ePTFE/SIS). This gave a total of five samples of each mesh at each study time, each mesh sample being recovered from a different animal.

### **Surgical technique**

All animals were given 0.05 mg/kg buprenorphine 1 hour before surgery to minimize pain. The animals were anesthetized using a mixture of ketamine chlorohydrate (Ketolar, Parke-Davis, Barcelona, Spain) (70 mg/kg); diazepam (Valium, Roche, Madrid, Spain) (1.5 mg/kg); and chlorpromazine (Largactil, Rhone-Poulenc, Madrid, Spain) (1.5 mg/kg) administered intramuscularly.

Two longitudinal incisions some 5-cm long were made on either side of the midline. Next, two musculofascial defects (3 x 3 cm) were created on the oblique muscle (sparing the transverse muscle and parietal peritoneum) (Figure 1A and B). Each animal was implanted with two prostheses, ePTFE/SIS or Coll/Pe. Prior to their implant, SIS and Coll were hydrated using saline as indicated in the manufacturers' instructions.

Each prosthesis was fixed to the edges of the defect by a running 4/0 polypropylene suture, which was interrupted at the four corners (Figure 1C–F). The skin was closed over the defects by running 3/0 polypropylene suture.

During the study period and before the time of sacrifice, the animals were visually inspected to check for signs of dehiscence of the skin wound, seroma formation, wound infection, and/or mesh incompatibility.

At each of the established time points, 14, 30, 90, and 180 days after implant, 10 animals were sacrificed in a CO<sub>2</sub> chamber.

### **Prosthetic shrinkage**

After sacrificing the animals, the implants were excised by making an incision around the mesh that included a large margin of surrounding host tissue. Shrinkage was determined by tracing the shape of the implant on a transparent polyvinyl template just before mesh removal. Next, the surface area of the implant outline was determined by image analysis, digitalizing the images of the implants obtained using the Medical Image Processing (MIP) program incorporated in the image analyzer (MICRON, Barcelona, Spain).

### **Morphological analyses**

After their visual inspection, the biomaterials were processed for light microscopy by fixing in F13 fixative solution (60% ethanol, 20% methanol, 7% polyethylene glycol 300, and 13% distilled water), embedding in paraffin and sectioning into 5- $\mu$ m thick slices. The prepared sections were stained with hematoxylin and eosin and Masson's trichrome (Goldner-Gabe).

### **Immunofluorescence technique**

For immunofluorescence analysis, fixed specimens were embedded in paraffin and cut into 5- $\mu$ m thick sections. The sections were deparaffinated, hydrated, equilibrated in PBS buffer, and incubated, during 1 hour at 37 °C, with mouse monoclonal anticollagen type I antibody, clone COL-I (C2456; Sigma, St. Louis, MO) (1 : 400) and with mouse monoclonal antibody to type III collagen (hCL(III), clone III-53 (AF-5850; Medicorp, Montreal, Canada) (1 : 500). An immunofluorescence technique was used to detect the antigen-antibody reaction. A secondary antibody antimouse rhodamine conjugated (715-295-150; Jackson ImmunoResearch, Suffolk, UK) (1 : 300) was used for incubation in darkness for 1 hour at 37 °C. Cell nuclei were counterstained with 4',6-diamidino-2-phenylindole (DAPI). Samples were examined under a confocal microscope Leica SP5 (Leica Microsystems, Wetzlar, Germany) to detect fluorescence. DIC images were also obtained using this microscope. These images were merged with the fluorescence images to differentiate the newly formed collagen in the repair tissue from that of the biological prosthesis.

### **Quantitative-reverse transcription-polymerase chain reaction (q-RT-PCR)**

Total RNA was isolated from tissue samples embedded in paraffin using the kit Absolutely RNA FFPE (Agilent Technologies, Santa Clara, CA) according to the manufacturer's instructions. Ten sections per specimen including the area of the biological prosthesis and neoformed host tissue were used for RNA extraction. The kit includes a DNase treatment step to avoid DNA contamination. Reverse transcription was carried out as described previously.<sup>14</sup> mRNA expression was determined by q-RT-PCR using the Standard Curve program in a StepOnePlus Real-Time PCR System Applied Biosystem instrument (Applied Biosystems, Foster City, CA). iQ SYBR Green Supermix was used following the manufacturer's instructions (Bio-Rad Laboratories, Hercules, CA). A negative control containing DNase- and RNase-free ultraPure™ distilled water (Invitrogen, Carlsbad, CA) was run alongside each reaction. Primers were designed by our group using Primer Express software, version 3.0 (Applied Biosystems, Foster City, CA). The specific rabbit primers used for amplification were: Col 1a1 gene: 5'-ATA GAG

GAC CAC GTG GAG AAA GG-3 (sense) and 5'-CCG TTG GGA CCA TCA TCA C-3' (antisense); Col 3a1 gen: 5'-CAT TGG CCC TGT TTG CTT TTT A-3' (sense) and 5'-TGA CAA GAT TAG AAC AAA AGC AAC ACA-3' (antisense); glyceraldehyde 3-phosphate-dehydrogenase (GAPDH): 5'-ACA ACT CTC TCA AGA TTG TCA GCA A-3' (sense) and 5'-GCC GAA GTG GTC GTG GAT-3' (antisense). The thermal cycling conditions were: an initial stage at 95 °C for 10 minutes, followed by 50 cycles of 95 °C for 15 seconds, 60 °C for 30 seconds, and 72 °C for 1 minute. Products were checked by 2% agarose gel electrophoresis and visualized with ultraviolet light. Gene expression was normalized against the expression of the constitutive gene GAPDH.

### **Biomechanical resistance**

To assess the stress resistance of the different biomaterials, the tensile strengths of strips, 2 cm x 5 cm, comprising the prostheses and the sutures used to fix the implants to the host tissue at each end of the strips, were determined using a tensiometer model INSTRON 3340 (static load cell 500N) (Instron Corp., Marlow, UK). The crosshead speed was 5 cm/minute and recording speed 2 cm/minute. All measurements were made immediately after the animals had been sacrificed at 14, 30, 90, and 180 days postimplant.

### **Statistical analysis**

All data are expressed as mean± standard error of measurement. The Mann–Whitney test was used to compare data among the different study groups. The level of significance was set at  $p < 0.05$ . All statistical analyses were performed using the GraphPad Prism 4 package (GraphPad Inc., La Jolla, CA).

## **RESULTS**

### **In vivo study**

All rabbits were examined for abscess formation, surgical site infection, presence of seroma and hematoma, fistulae, or extrusion of the graft material.

Seroma was the most common complication noted. Among the control animals with an ePTFE implant, five animals had seroma and one animal had skin dehiscence. The Coll group also contained five animals with seroma, along with one animal with skin dehiscence, and another with a cutaneous fistula. In the group Pe, there were three cases of seroma, and in SIS, we observed two cases of mesh detachment from the cutaneous bed and five animals with seroma.

### **Prosthetic shrinkage**

Pe and Coll were the implants that suffered least shrinkage, while the ePTFE and SIS groups showed the largest mean % shrinkage values (Figures 2 and 3).

Within the SIS group, a significant difference was detected between the shrinkage values recorded at 14 days and at 90/180 days. Shrinkage in these implants peaked at 14 days and thereafter gradually decreased until the end of the study. In the ePTFE group, mean percentage shrinkage values at 90days differed significantly from those recorded at 14/30 days.

The Coll and Pe implants showed similar surface areas throughout the study (Figure 3).



When shrinkage percentages in the different implants were compared at a given time point, it was noted that at 14 and 30 days, ePTFE and SIS suffered significantly greater shrinkage than the rest of the prostheses. However, in the mid/long term, at 90 and 180 days, only in the ePTFE group did significant differences with the rest of the groups persist (Figure 3).

### **Morphological analyses**

In general, no cell infiltration inside the biomaterial was observed in the ePTFE group, while in the collagen meshes, neoformed connective tissue and inflammatory cells were seen to penetrate the implant interior.

The ePTFE implants became encapsulated by a fibrous neoformed tissue that was highly cellular and contained numerous blood vessels at all the time points. The lack of porosity of this type of prosthesis (Preclude) prevented the ingrowth of cells in the prosthetic material. On both sides, subcutaneous and muscular, the cells formed an uninterrupted barrier around the implant (Figure 4A and E).

The histological behavior of the two cross-linked prostheses (Coll and Pe) was similar. Already at 14 days, differences could be observed in the host response to the implants compared with the ePTFE. A fibrous capsule formed on both surfaces of the prosthesis and cells lined its perimeter. However, a large number of the same cell types could also be seen in the interior of the biomaterials. Areas of neoformed connective tissue expanded over the study period from the outer prosthetic zone toward the inside, their presence being more intense in the greater irregularities of the material. In these groups, neoformed connective tissue density increased and small blood vessels appeared. Cell colonization was limited to the outermost third of the meshes. At this time point, signs of degeneration of the implanted collagen and its gradual replacement by host tissue were starting to emerge (Figure 4B, C, F, and G).

The structure of SIS consisting of separate layers of collagen considerable conditioned the remodeling process. Thus, it was the SIS implant that generated the greatest inflammatory reaction. At 14 days, the presence of abundant granulation tissue comprised of lymphocytes, macrophages, and polymorphonuclear cells became evident (Figure 4D). These cells managed to squeeze between the collagen sheets occupying the entire SIS mesh thickness. At 30 days, the inflammatory reaction was more intense and collagen fibers appeared more separated by inflammatory cells than at 14 days. Prosthetic colonization continued until the later time points (90/180 days) when a considerable increase in neoformed connective tissue was observed, along with an evidently diminished inflammatory process and reduced initial thickness of the collagen layers. These processes constitute the degeneration of the material and its gradual replacement by host tissue. In the long term (180 days), the degradation of the biological prostheses was almost complete and in their place a highly vascular regeneration neotissue had formed (Figure 4H).

### **Immunofluorescence technique**

The immunofluorescence confocal microscopy images were superimposed on the DIC images, so the newly formed collagens in the neotissue, identified using the corresponding antibody (anticollagen I or III), appear as red immunofluorescence and the native collagens forming the prostheses appear translucent.

Fourteen and 30 days after placement, the different types of prostheses showed sparse



or no immunostaining for collagen type I (mature collagen) (Figure 5A–D). The levels of this protein increased over time, such that at 90 and 180 days the different samples showed peak staining (Figure 5E–H).

In the ePTFE group, staining was limited to the tissue encapsulating the prosthesis (Figure 5E). In the Coll and Pe groups, maximum staining for collagen I was observed at 90 and 180 days and was localized in the fibrous connective tissue surrounding the prosthesis and in some tissue areas that penetrated the material (Figure 5F and G). In the SIS implants, staining was more discrete and evenly distributed throughout the biomaterial's thickness at 90 and 180 days (Figure 5H).

For collagen type III, the immunostaining pattern was completely different to that observed for collagen I. At 14 days postimplant, collagen type III was highly expressed in the neoformed tissue, and this expression rose at 30 days and continued increasing in the mid and long term (Figure 6).

In the control group, collagen III appeared as bands parallel to the ePTFE implants that increased in thickness over time (Figure 6A and E). In the Coll and Pe groups, collagen III infiltrated the material, which showed some cell nuclei within it at 90 and 180 days (Figure 6B and F, and C and G).

In the SIS biological meshes, large areas of neoformed tissue appeared which showed expression for this collagen type. The disappearance of the prosthetic material with increasing implant time was remarkable (Figure 6D and H). In the long term, the absence of the native prosthetic material was notable indicating its complete degradation and tissue regeneration in the area (Figure 6H).

#### **q-RT-PCR**

In the Coll and Pe groups, collagen 1a1 mRNA overexpression was detected at 14 days postimplant differing significantly from the expression noted at the remaining study times. Thus, early after implant, the cells surrounding and colonizing these two meshes caused significant up-regulation of collagen 1a1 gene expression. At 30 days, both groups showed significantly reduced expression levels that rose slightly at 90 days as the amount of host tissue in the implant increased (Figure 7A and B).

In the ePTFE group, the observation of relatively higher collagen 1a1 mRNA levels was delayed until 90 days compared with the Coll and Pe groups, with a significant increase in expression produced with respect to 14 and 180 days (Figure 7D).

The SIS group implants showed little collagen 1a1 mRNA expression, and no significant differences were observed for the different time points (Figure 7C).

The gene expression of collagen 3a1 in Coll and Pe showed the same pattern of expression to that of collagen 1. In both groups, collagen 3a1 mRNA expression was detected at 14 days postimplant at levels that differed significantly to those recorded at the remaining study times. At 30 days, expression levels were significantly lower in both groups with respect to the previous study time and this difference persisted in the Coll group throughout the study. In the Pe group, collagen 3a1 mRNA expression at 90 days was significantly higher than the level recorded at 30 days yet was also significantly reduced at 180 days (Figure 7A and B).

SIS showed a very different pattern of collagen 1a1 gene expression. In this group, collagen 3a1 mRNA expression rose to significantly higher levels observed at 90 days postimplant with respect to the previous study times but not to the later time point. Significant differences were also observed between the earliest and latest time points

(Figure 7C).

The ePTFE implants showed very little collagen 3a1 mRNA expression at all the study times with no differences detected between them (Figure 7D).

### **Biomechanical resistance**

For each of the implants, lowest tensile strengths were recorded at 14 days and thereafter they gradually gained in strength. In the Pe and Coll groups, the tensile strengths recorded at each of the time points differed significantly among each other.

When the biomechanical resistances of the different prostheses were compared by time point, highest values at 14 days were recorded for Coll, which differed significantly to the values recorded for Pe and SIS. At 30 days, this same group continued to show significantly higher tensile strengths than Pe, with differences also detected between Pe and ePTFE. In the mid/long term, Coll still showed significant differences with SIS alone, and at 180 days, it was the control ePTFE group whose tensile strengths were significantly lower than the strengths recorded for the two cross-linked meshes (Pe and Coll) (Figure 8).

### **DISCUSSION**

The ultimate goal of a biological prosthesis is to achieve good host tissue ingrowth while minimizing the tissue reaction produced by remodeling host tissue. Remodeling is a term used to describe native tissue ingrowth into a biological prosthesis. It implies the replacement of the implanted or foreign tissue with host tissue.<sup>15</sup>

Using staining techniques, it is practically impossible to distinguish the prosthesis from newly formed tissue once the remodeling process has started.<sup>8,16</sup> The immunofluorescence confocal microscopy/DIC technique used in the present study enabled us to clearly differentiate between the collagen comprising the implanted mesh and the collagen synthesized and secreted by the host cells that invade and replace these biological prostheses. The depth of cell infiltration into the acellular tissue decreases with an increasing extent of cross-linking such that this factor determines the degradation rate of the acellular biomaterial and its tissue regeneration pattern.<sup>17</sup> This rationale is consistent with our observations in the different biomaterials. Cross-linking constitutes an effective barrier against enzyme degradation.<sup>8</sup> Thus, noncross-linked prostheses run the risk of being too rapidly degraded by proteases secreted by infiltrated inflammatory cells before fibroblasts migrating from the host tissue have had the time to secrete their own extracellular matrix.

The noncross-linked SIS prosthesis examined here appeared highly degraded 180 days after implant, in agreement with the absence of SIS used to repair abdominal wall defects in dogs observed after 4 months.<sup>18</sup> Other authors<sup>19</sup> have recently tested the use of a similar prosthesis (InteXen LP, American Medical Systems, Inc, Minnetonka, MN) to repair fascial defects in a rat model. These authors described remodeling of the implant site by 180 days without compromising stress resistance and also noted the greater tensiometric strength of noncross-linked prostheses. In our tests, however, SIS elicited the greatest extent and fastest rate of remodeling, yet stress resistance was significantly compromised. We were able to correlate this with larger amounts of collagen type III involved in remodeling at the expense of collagen type I, as responsible for the mechanical properties of the neoformed tissue. In addition, the intense

inflammatory reaction induced by a noncross-linked mesh will contribute to prosthetic degradation with the consequent reduction in biomechanical resistance, as was observed in our SIS group in the short term. The ensuing rapid replacement of the native prosthesis with poorly structured host connective tissue explains the diminished mechanical resistance observed in SIS at 90 and 180 days postimplant.

In our ePTFE implants, the lack of good tissue ingrowth was reflected by low tensile strength measurements, in accordance with the findings of others.<sup>20</sup> In contrast, the cross-linked meshes examined induced both collagen I and III protein synthesis and deposition in the neoformed tissue. Our findings revealed collagen III protein expression early after implant (14 days) and delayed collagen I deposition until 90 days. Collagen 3a1 mRNA was overexpressed in both groups at the early implant stages. Collagen 1a1 showed a similar expression pattern although its protein expression was delayed up until 90 days, probably because of a longer translation and posttranslation process. Consequently, for both cross-linked prostheses, tissue remodeling was slower but the newly formed tissue was of better quality and biomechanical resistance was accordingly less compromised. In our model, cell and blood vessel infiltration into the prostheses were also scored in the histological sections (data not shown). Similar extents of both variables were observed at 180 days in the two cross-linked prostheses (Pe and Coll), showing significantly lower scores when compared with the SIS group. Hence, the capacity of this noncross-linked prosthesis to promote early cellular and vascular infiltration was in contradiction with its biomechanical behavior because the process was too fast to allow the formation of a well-structured replacement tissue whereby optimal synthesis and deposition of collagen occurs (mainly type I, which helps to modulate and give strength to the repair zone), as shown in the results.

In a recent short-term study,<sup>21</sup> significantly greater tensile strengths and mean cell and vessel densities were described for noncross-linked implants. This finding is inconsistent with our biomechanical results and possibly attributable to the fact that the noncross-linked prosthesis used (Strattice, LifeCell Corporation, Branchburg, NJ) was nonlaminar, thicker, and more compact than SIS. Such noncross-linked biological meshes, which are more slowly degraded, seem to offer early clinical advantages.

It has been reported<sup>22</sup> that extensive cross-linking of native matrix components results in prosthetic tissue damage and loss of the biological signals that promote remodeling. In turn, deficient signaling may inhibit host fibroblast infiltration into the material and angiogenesis within the matrix. This could explain the lack of recellularization of some cross-linked meshes in agreement with literature results.<sup>23</sup>

In a model of ventral hernia repair in the rat,<sup>15</sup> the persistence of implanted Permacol in the long term was described, cell ingrowth and neovascularization being visible by 3 months. This observation is consistent with our 6-month observations. In a recent pilot study<sup>22</sup> in primates using three types of porcine-derived biological meshes, a significant and immediate inflammatory foreign body response and impaired wound healing and tissue integrity were observed at 6 months. Also, one of the few experimental studies conducted in the rabbit indicates the complete remodeling of SIS 60 days after implant in pelvic floor surgery. The authors warn that the main problem related to the use of SIS is herniation caused by weakness of the repaired zone and recommend caution when SIS is used in high-tension zones such as the abdominal wall.<sup>24</sup> Other authors have, nevertheless, observed using noncross-linked prostheses, substantial collagen synthesis with good tissue organization and a less pronounced inflammatory response compared with that

induced by synthetic materials.<sup>25,26</sup>

Mesh shrinkage is still an unresolved problem in hernia repair. Conventional prosthetics are passive and, as a result, induce poor tissue ingrowth and shrinkage, which may be contributing factors for hernia recurrence and patient discomfort. In general terms, our prosthetic shrinkage results indicate less shrinkage suffered by Pe and Coll compared with ePTFE and SIS. In the early postimplant period, ePTFE and SIS showed significantly greater shrinkage than the remaining meshes, and in the long term, the synthetic prosthesis maintained its significant difference with the rest of the implants. Few researchers have addressed the issue of prosthetic shrinkage. In abdominal wall implants in the rat, Gaertner et al.<sup>15</sup> showed the absence of shrinkage in Pe at 6 months, while noncross-linked prostheses suffered significant prosthetic shrinkage. Another study<sup>22</sup> revealed that Coll, Pe, and SIS grafts all experience considerable shrinkage, concurring with other alterations in Pe and Coll such as pleating, bulging, and graft hardening. However, the SIS and Coll grafts shrunk significantly more than Pe during the implant course from 1 to 6 months. Rauth et al.<sup>20</sup> reported significantly more shrinkage in SIS than ePTFE when the biomaterials were sutured to the peritoneal surface.

Collectively, all these data suggest that the main benefit of a biological prosthesis over a synthetic prosthetic material is that, once implanted in the host, the collagen constituting the mesh will gradually degrade over time and become replaced with new collagen synthesized by host cells. The key to success therefore depends on the prosthetic degradation process not being too quick and also on the accompanying synthesis of new good quality tissue to gradually replace the prosthetic tissue. This remodeling should also fail to compromise the tensile strength properties of the repair zone. Thus, it seems that to control this prosthetic biodegradation process, the extent of cross-linking needs to be modulated.

The main conclusions of our study are:

- (1) Collagen prostheses devoid of cross-links allow better cell and tissue ingrowth and are therefore more rapidly degraded than their cross-linked counterparts.
- (2) In the long term, the tensile strength of a cross-linked collagen implant is significantly greater than that of an ePTFE prosthesis.
- (3) In the early implant stages, cross-linked collagen implants induce the up-regulation of collagen 1 $\alpha$ 1 and 3 $\alpha$ 1 gene expression in the host, which translates to a steady increase in the presence of both proteins over time.

Collagen cross-linked biological prostheses thus seem to be a good alternative to synthetic prosthetic materials in that they promote slow tissue ingrowth, provide strength to the abdominal wall, and avoid prosthetic shrinkage. Further improvements such as modifying the extent of cross-linking could serve to promote better host tissue incorporation.

## **ACKNOWLEDGMENTS**

This study was supported by a grant from the Fundación Mutua Madrileña 2008 (FMM08), Madrid, Spain, and by the Spanish Ministry of Science and Technology through the research project DPI2011-27939. The authors confirm that there are no known conflicts of interest associated with this publication, and there has been no significant financial support for this work that could have influenced its outcome.

## REFERENCES

1. Binnebösel M, von Trotha KT, Jansen PL, Conze J, Neumann UP, Junge K. Biocompatibility of prosthetic meshes in abdominal surgery. *Semin Immunopathol* 2011; 33: 235–43.
2. Bellows CHF, Alder A, Helton WS. Abdominal wall reconstruction using biological tissue grafts: present status and future opportunities. *Expert Rev Med Devices* 2006; 3: 657–75.
3. Badylak SF, Kropp B, McPherson T, Liang H, Snyder P. Small intestine submucosa: a rapidly resorbed bioscaffold for augmentation cytoplasty in a dog model. *Tissue Eng* 1998; 4: 379–87.
4. Abraham GA, Murray J, Billiar K, Sullivan SJ. Evaluation of the porcine intestinal collagen layer as biomaterial. *J Biomed Mater Res* 2000; 51: 442–52.
5. Klinge U, Klosterhalfen B, Muller M. Shrinking of polypropylene mesh in vivo: an experimental study in dogs. *Eur J Surg* 1998; 164: 965–99.
6. Schachtrupp A, Klinge U, Junge K, Roch R, Bhardway RS, Schumpelick V. Individual inflammatory response of human blood monocytes to mesh biomaterials. *Br J Surg* 2003; 90: 114–20.
7. Menon NG, Rodríguez ED, Bymes CK, Girotto JA, Goldberg NH, Silverman RP. Revascularization of human acellular dermis in full-thickness abdominal wall reconstruction in the rabbit model. *Ann Plast Surg* 2003; 50: 523–7.
8. Liang HCH, Chang Y, Hsu CHK, Lee MH, Sung HW. Effects of crosslinking degree of an acellular biological tissue on its tissue regeneration pattern. *Biomaterials* 2004; 25: 3541–52.
9. Bellón JM, Buján J, Contreras LA, Carrera-San Martín A. Comparison of a new type of polytetrafluoroethylene patch (MycroMesh) and polypropylene prosthesis (Marlex) for repair of abdominal wall defects. *J Am Coll Surg* 1996; 183: 11–8.
10. Bellón JM, Contreras LA, Buján J, Palomares D, Carrera-San Martín A. Tissue response to polypropylene meshes used in the repair of abdominal wall defects. *Biomaterials* 1998; 19: 669–75.
11. Catena F, Ansaloni L, Gazzotti F, Gagliardi S, Di Saverio S, D'Alessandro L, Pinna AD. Use of porcine dermal collagen graft (Permacol) for hernia repair in contaminated fields. *Hernia* 2007; 11: 57–60.
12. Franklin ME, Treviño JM, Portillo G, Vela I, Glass JL, González JJ. The use of porcine small intestinal submucosa as a prosthetic material for laparoscopic hernia repair in infected and potentially contaminated fields: long-term follow-up. *Surg Endosc* 2008; 22: 1941–6.
13. Bachman S, Ramshaw B. Prosthetic material in ventral hernia repair: how do I choose? *Surg Clin North Am* 2008; 88: 101–12.
14. Pascual G, Rodríguez M, Gomez-Gil V, García-Honduvilla N, Buján J, Bellón JM. Early tissue incorporation and collagen deposition in lightweight polypropylene meshes: bioassay in an experimental model of ventral hernia. *Surgery* 2008; 144: 427–35.
15. Gaertner WB, Bonsack ME, Delaney JP. Experimental evaluation of four biologic prostheses for ventral hernia repair. *J Gas-trointest Surg* 2007; 11: 1275–85.
16. Badylak S, Kokini K, Tullius B, Simmons-Byrd A, Morff R. Morphologic study of small intestinal submucosa as a body wall repair device. *J Surg Res* 2002; 103: 190–202.
17. Huang LL, Sung HW, Tsai CC, Huang DM. Biocompatibility study of a biological tissue fixed with a naturally occurring crosslinking reagent. *J Biomed Mater Res* 1998; 15:



568–76.

18. Clarke KM, Lantz GC, Salisbury SK, Badylak SF, Hiles MC, Voytik SL. Intestine submucosa and polypropylene mesh for abdominal wall repair in dogs. *J Surg Res* 1996; 60: 107–14.
19. Ozog Y, Konstantinovic M, Zheng F, Spelzini F, Verbist G, Luyten C, De Ridder D, Deprest J. Porous acellular porcine dermal collagen implants to repair fascial defects in a rat model: biomechanical evaluation up to 180 days. *Gynecol Obstet Invest* 2009; 68: 205–12.
20. Rauth TP, Poulose BK, Nanney LB, Holzman MD. A comparative analysis of expanded polytetrafluoroethylene and small intestinal submucosa—implications for patch repair in ventral herniorrhaphy. *J Surg Res* 2007; 143: 43–9.
21. Butler CE, Burns NK, Campbell KT, Mathur AB, Jaffari MV, Rios CN. Comparison of cross-linked and non-cross-linked porcine acellular dermal matrices for ventral hernia repair. *J Am Coll Surg* 2010; 211: 368–76.
22. Sandor M, Xu H, Connor J, Lombardi J, Harper JR, Silverman RP, McQuillan DJ. Host response to implanted porcine-derived biologic materials in a primate model of abdominal wall repair. *Tissue Eng Part A* 2008; 14: 2021–31.
23. Petter-Puchner AH, Fortelny RH, Walder N, Mittermayr R, Ohlinger W, van Griensven M, Redl H. Adverse effects associated with the use of porcine cross-linked collagen implants in an experimental model of incisional hernia repair. *J Surg Res* 2008; 145: 105–10.
24. Claerhout F, Verbist G, Verbeken E, Konstantinovic M, De Ridder D, Deprest J. Fate of collagen-based implants used in pelvic floor surgery: a 2-year follow-up study in a rabbit model. *Am J Obstet Gynecol* 2008; 198: 94–6.
25. Konstantinovic ML, Lagae P, Zheng F, Verbeken EK, De Ridder D, Deprest JA. Comparison of host response to polypropylene and non-cross-linked porcine small intestine serosal-derived collagen implants in a rat model. *BJOG* 2005; 112: 1554–60.
26. Rice RD, Ayubi FS, Shaub ZJ, Parker DM, Armstrong PJ, Tsai JW. Comparison of Surgisis, AlloDerm, and Vicryl Woven Mesh grafts for abdominal wall defect repair in an animal model. *Aesthetic Plast Surg* 2010; 34: 290–6.



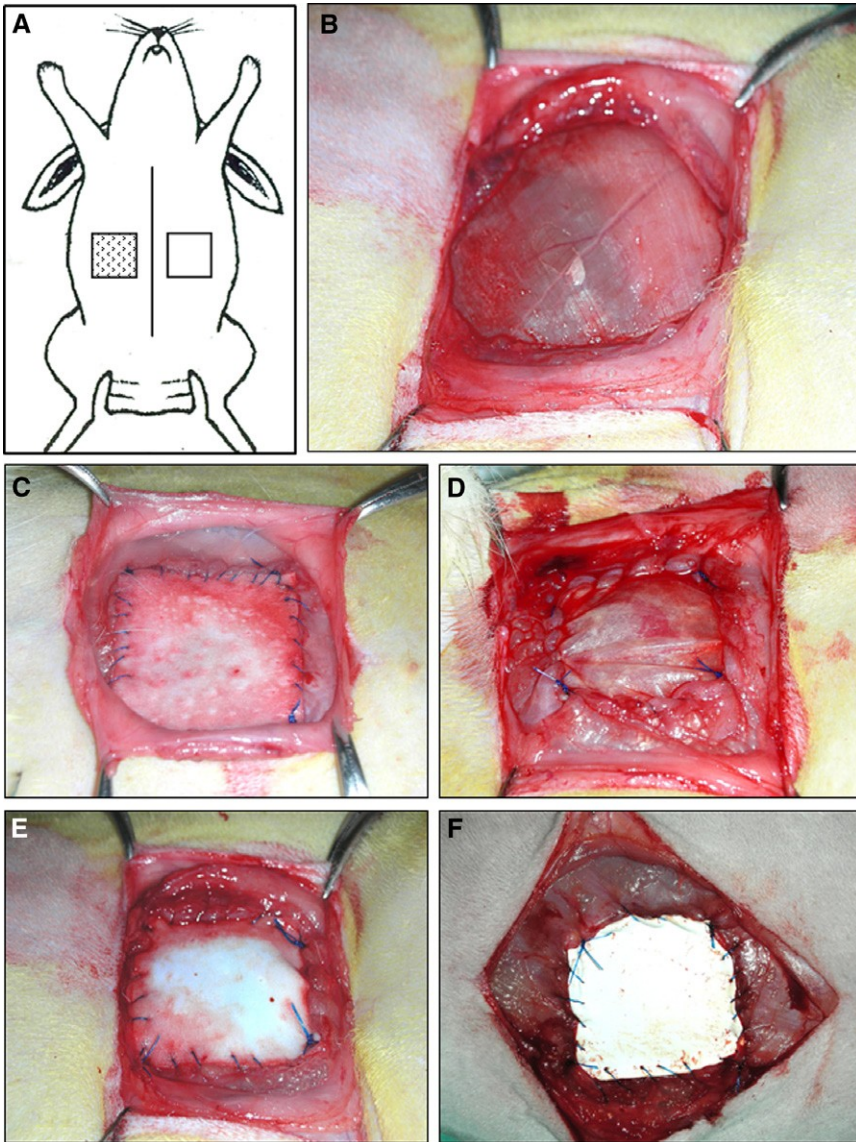


**Figure 1.** (A) Experimental design; (B) image of the defects (3 x3 cm) created in the anterior abdominal wall of New Zealand rabbits leaving the transverse muscle and peritoneum intact; (C) CollaMend; (D) Surgisis; (E) Permacol; (F) expanded polytetrafluoroethylene implants.

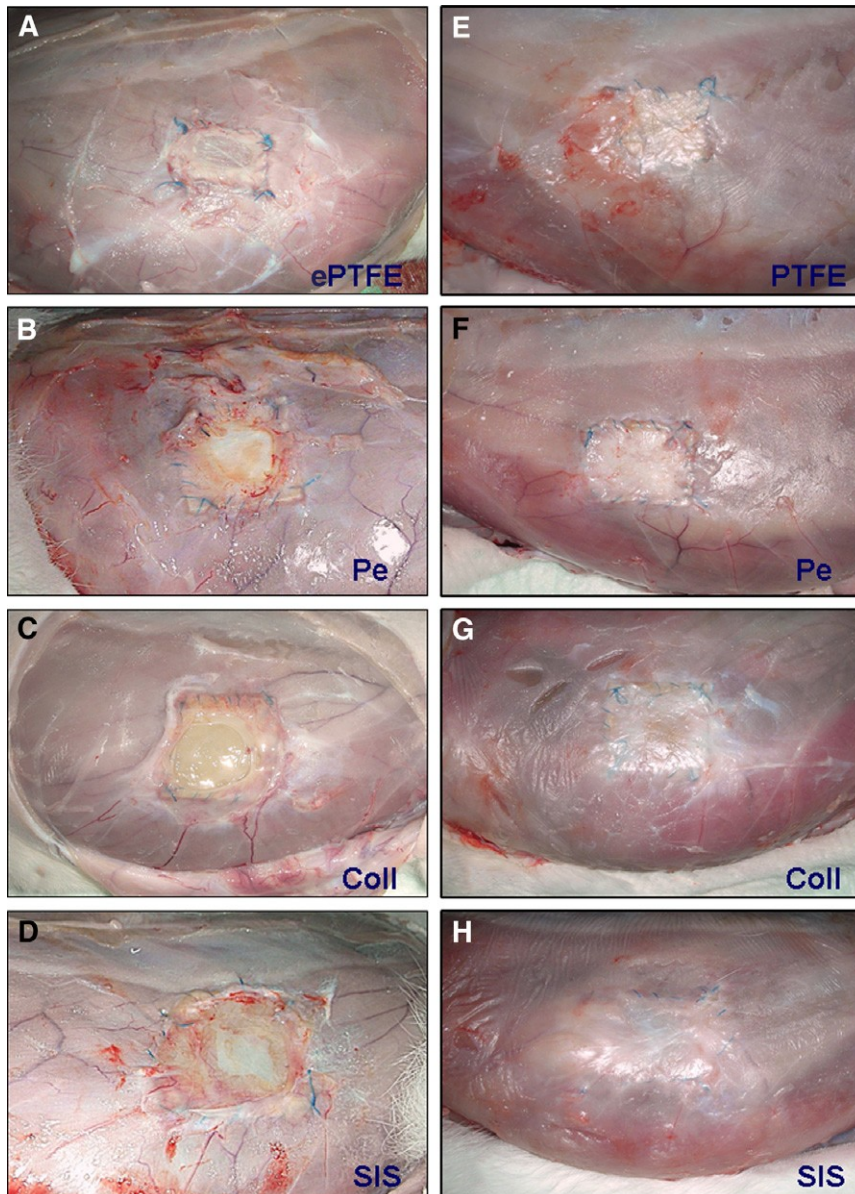


**Figure 2.** Macroscopic view of the different biomaterials at 30 (A–D) and 180 (E–H) days postimplant. ePTFE, expanded polytetrafluoroethylene; PE, Permacol; Coll, CollaMend; SIS, Surgisis.

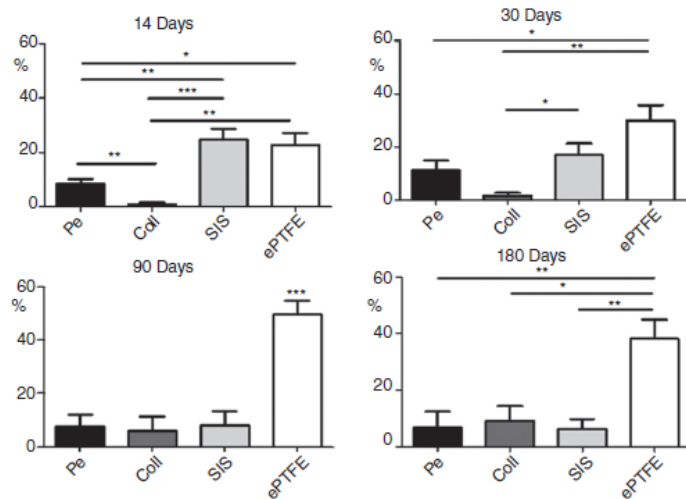


**Figure 3.** Percentage shrinkage values for the four implanted biomaterials at the different study times (\* $p < 0.05$ ; \*\* $p < 0.01$ ; \*\*\* $p < 0.005$ ). ePTFE, expanded polytetrafluoroethylene; PE, Permacol; Coll, CollaMend; SIS, Surgisis.



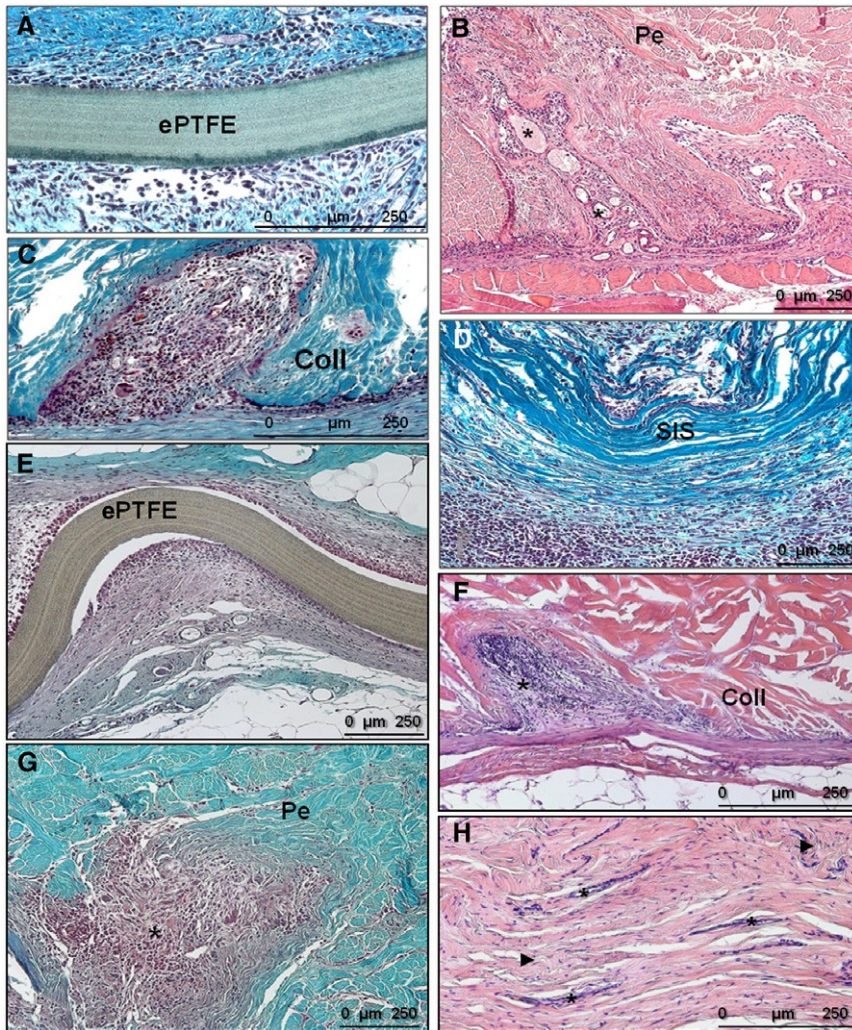


**Figure 4.** (A) Control group. ePTFE 30 days (Masson's trichrome staining; 200x); (B) detail showing tissue infiltration with intense angiogenesis (\*) within Pe at 30 days (hematoxylin & eosin staining; 100x); (C) Coll, 30 days, neoformed connective tissue and inflammatory cells penetrating the pores of the Coll to completely fill them (Masson's trichrome staining; 200x); (D) SIS 14 days (Masson's trichrome staining; 100x); inflammatory cells infiltrating the collagen filaments, both in the interior and periphery of SIS. (E) Control group. ePTFE after 180 days showing encapsulation of the prosthesis (Masson's trichrome staining; 100x); (F) Coll, 180 days postimplant (hematoxylin & eosin staining; 160x), (\*) tissue infiltration; (G) tissue infiltration (\*) observed in Pe at 180 days (Masson's trichrome staining; 100x); (H) neoformed connective tissue in SIS after 180 days postimplant showing intense angiogenesis (\*) and only traces of the prosthesis (▶) (hematoxylin & eosin staining; 160x). ePTFE, expanded polytetrafluoroethylene; PE, Permacol; Coll, CollaMend; SIS, Surgisis.



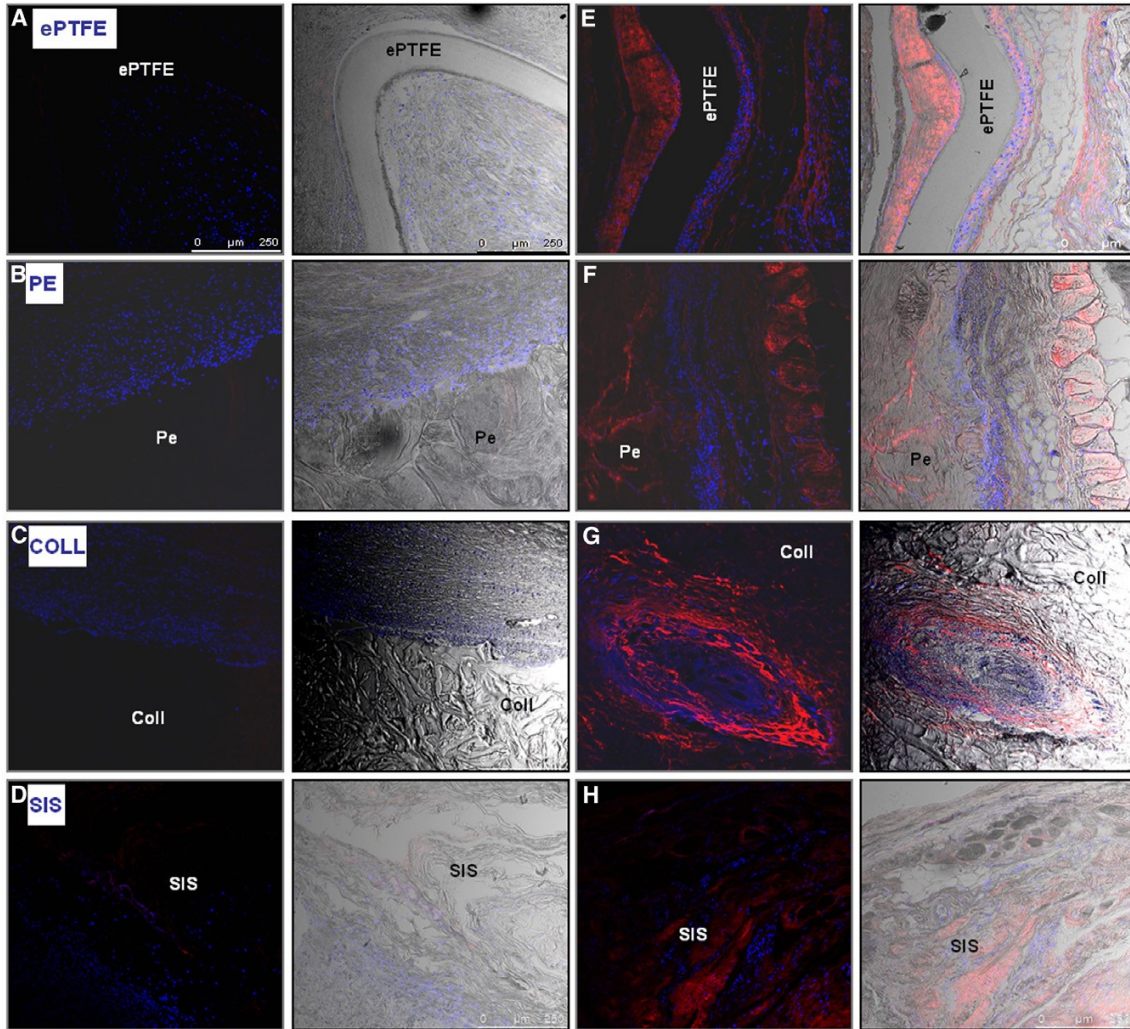


**Figure 5.** Immunofluorescence detected expression of collagen I in the different study groups at 30 (A–D) and 90 days (E–H) postimplant. ePTFE (A and E), Pe (B and F), Coll (C and G), and SIS (D and H). Confocal laser microscopy (100x). Images on the right show the same fluorescence image merged with the DIC images to identify the collagen comprising the prosthetic material. Collagen expression appears red, cell nuclei appear blue (DAPI), and the collagen that forms the biological prosthesis appears translucent. ePTFE, expanded polytetrafluoroethylene; PE, Permacol; Coll, CollaMend; SIS, Surgisis; DIC, differential interference contrast; DAPI, 4'6-diamidino-2-phenylindole.

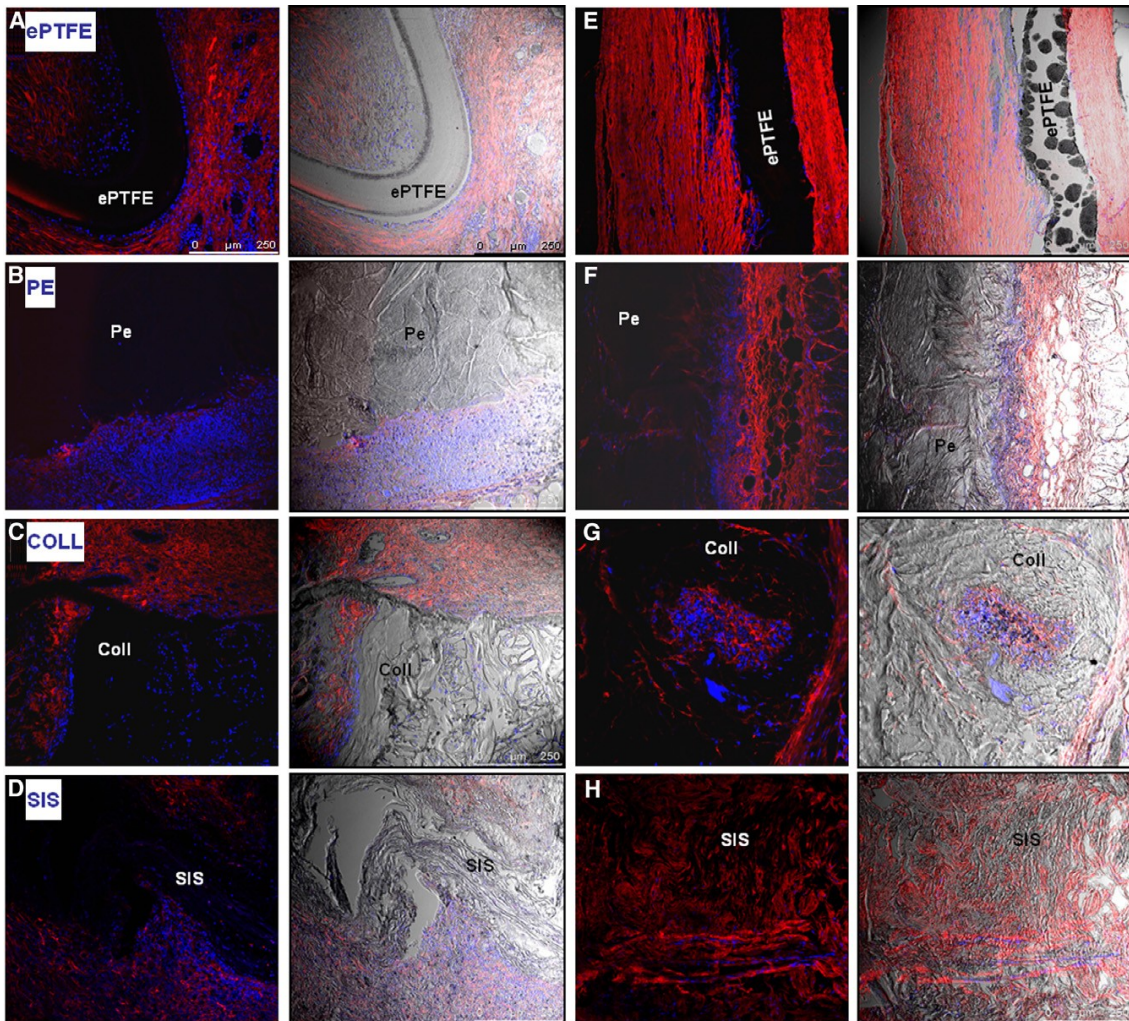


**Figure 6.** Immunofluorescence detected expression of collagen III in the different study groups at 30 (A–D) and 90 days (E–H) postimplant. ePTFE (A and E), Pe (B and F), Coll (C and G), and SIS (D and H). Confocal laser microscopy (100x). Images on the right show the same fluorescence image merged with the DIC images to identify the collagen comprising the prosthetic material. Collagen expression appears red, cell nuclei appear blue (DAPI), and the collagen comprising the biological prostheses appears translucent. ePTFE, expanded polytetrafluoroethylene; PE, Permacol; Coll, CollaMend; SIS, Surgisis; DIC, differential interference contrast; DAPI, 4′6-diamidino-2-phenylindole.



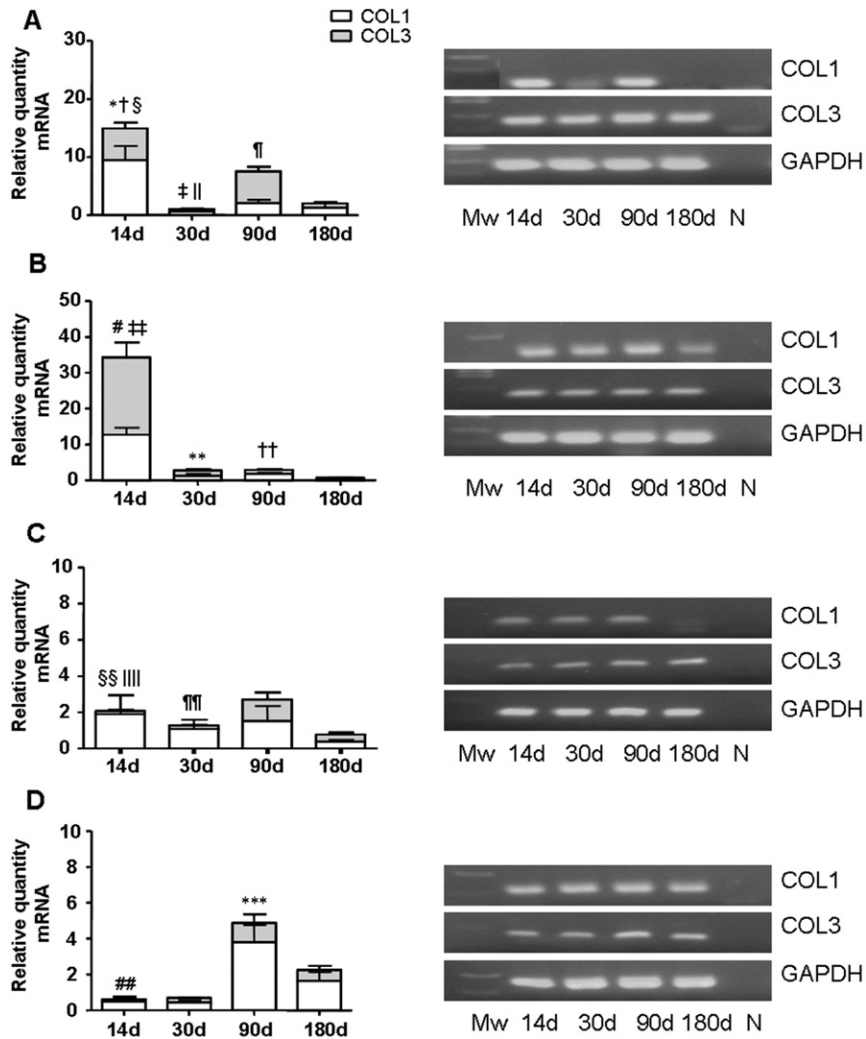


**Figure 7.** Col 1a1 and Col 3a1 mRNA expression. (A) Permacol: Col 1a1: \*,  $p < 0.01$  vs. 30 days; †,  $p < 0.05$  vs. 90/180 days; ‡,  $p < 0.05$  vs. 90 days. Col 3a1: §,  $p < 0.001$  vs. 30/180 days; ||,  $p < 0.0001$  vs. 90 days; ¶,  $p < 0.001$  vs. 180 days. (B) CollaMend: Col 1a1: #,  $p < 0.001$  vs. 30/90/180 days; \*\*,  $p < 0.05$  vs. 90/180 days; ††,  $p < 0.01$  vs. 180 days. Col 3a1: ‡‡,  $p < 0.001$  vs. 30/90/180 days. (C) Surgisis: Col 3a1: §§,  $p < 0.01$  vs. 90 days; ||||,  $p < 0.05$  vs. 180 days; ¶¶,  $p < 0.01$  vs. 90 days. (D) ePTFE: Col 1a1: ##,  $p < 0.05$  vs. 90 days; \*\*\*,  $p < 0.05$  vs. 180 days. Data expressed as mean  $\pm$  SEM. Right panel, RT-PCR products of the two genes (collagen 1a1 and 3a1) at the different study times. Gene expression was normalized against the expression of the constitutive gene GAPDH. Mw, molecular weight markers; N, negative control; ePTFE, expanded polytetrafluoroethylene; SEM, standard error of the mean; RT-PCR, reverse transcription-polymerase chain reaction, GAPDH, glyceraldehyde 3- phosphate dehydrogenase.

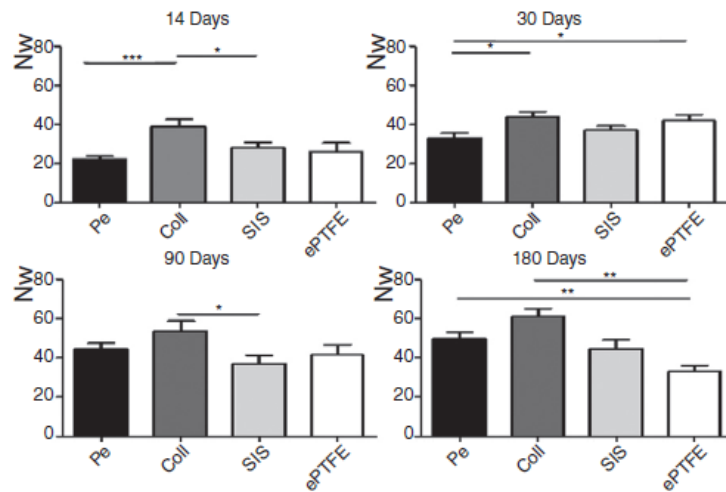


**Figure 8.** Biomechanical results for the four implanted biomaterials at 14, 30, 90, and 180 days postimplant in the different groups ( $*p < 0,05$ ;  $**p < 0.01$ ;  $***p < 0.005$ ). ePTFE, expanded polytetrafluoroethylene; PE, Permacol; Coll, CollaMend; SIS, Surgisis; Nw, Newtons.